IEEE Access
Multidisciplinary | Rapid Review | Open Access Journal

SPECIAL SECTION ON ENERGY MANAGEMENT IN BUILDINGS

Received May 17, 2018, accepted June 15, 2018, date of publication June 20, 2018, date of current version July 12, 2018.

Digital Object Identifier 10.1109/ACCESS.2018.2849094

Energy Efficient Learning-Based Indoor Multi-Band WLAN for Smart Buildings

XIAOYAN WANG[1], (Member, IEEE), MASAHIRO UMEHIRA[1], (Member, IEEE), HIROYUKI OTSU[2], TAKYUYA KAWATANI[3], AND SHIGEKI TAKEDA[1], (Member, IEEE)

[1]Graduate School of Science and Engineering, Ibaraki University, Hitachi 316-8511, Japan
[2]Mitsubishi Electric Corporation Energy System Center, Yokohama 220-0012, Japan
[3]KYOWA EXEO Corporation, Tokyo 150-0002, Japan

Corresponding author: Masahiro Umehira (masahiro.umehira.dr@vc.ibaraki.ac.jp)

This work was supported in part by the Japan Society for the Promotion of Science Grant-in-Aid for Young Scientists (B) under Grant 17K12670 and in part by Grant-in-Aid for Scientific Research (B) under Grant 18H01434A.

ABSTRACT Broadband Internet access in the building has fundamentally changed almost every aspect of our lives. As the growing use of indoor portable systems and devices, saving their energy consumption becomes an interesting and important issue for smart buildings. Recently, multi-band WLAN where 2.4/5-GHz and 60-GHz bands coexist is a promising solution to offer both ultra-high speed and robust wireless connections. For a multi-band WLAN end device, detecting the available service areas in an energy efficient way is of great importance. In the existing systems, the RF units of device need to be turned on and kept listening all the time, which leads to substantial energy consumption overhead. To solve this problem, this paper proposes an energy efficient learning-based indoor multi-band WLAN system, in which the end device predicts the distinct service areas by learning the influences of reflected waves in buildings. We have performed extensive experiments in different indoor environments, and the evaluation results demonstrate that the proposed mechanism could substantially improve the performance compared with the existing approaches.

INDEX TERMS Energy efficiency, multi-band WLAN, learning mechanism, indoor environment, smart building.

I. INTRODUCTION

In the smart buildings [1]–[3], in order to provide dedicated services and accurate management, the energy consumption issue [4]–[6] inside the building becomes critical. Recently, most of the works in energy management in smart buildings focus on the energy consumption of static sensors and actuators that are embedded into the walls and ceilings. However, the energy consumption of portable user devices inside the buildings, e.g., smartphone, tablet, wireless joystick, are mostly ignored. In fact, when running the bandwidth-hungry applications such as video streaming, virtual reality, or online games, the batteries of those end devices drain very fast, which leads to frequent charging and thus bad user experience. Since most of these portable devices connect into the Internet by WLANs (Wireless Local Area Networks), a smart energy efficient indoor WLAN system becomes a key component for the energy management in buildings.

Currently, to cope with the tremendous increases of wireless devices and data rate requirements in smart buildings, WLANs operating in 60GHz band are widely investigated. Specifically, it has been introduced as Wireless Gigabit (WiGig) [7], and standardized as IEEE 802.11ad [8]. WiGig aims to extend the Wi-Fi operation to the millimeter wave (mmWave) band. By using a 2.16GHz-width channel, it could provide bitrates upto 6.76Gbps. WiGig needs to use directional antennas due to the large free space path loss in 60GHz, and a countermeasure to combat severe shadowing loss caused by moving human body [9], [10].

Research issues on 60GHz band WLANs have attracted considerable attentions recently [11]–[14]. Theoretical analysis on the performance of IEEE 802.11ad mmWave WLAN has been done in [11] and [12]. Kushida *et al.* [13] addressed the frequent handover issue in IEEE 802.11ad due to the nature of mmWave and thus the small coverage. Kurniawan *et al.* [14] studied channel classification problem in IEEE 802.11ad system by using machine learning. In addition, the unique problems of 60GHz band WLAN in an indoor environment have also been investigated in [15]–[18].

2169-3536 © 2018 IEEE. Translations and content mining are permitted for academic research only.
Personal use is also permitted, but republication/redistribution requires IEEE permission.
See http://www.ieee.org/publications_standards/publications/rights/index.html for more information.

Saha *et al.* [15], [16] addressed the feasibility of using mmWave to build general purpose indoor WLANs. Yamada *et al.* [17] experimentally evaluated the throughput performance of off the shelf mmWave WLAN devices. Chen *et al.* [18] studied the optimal access point deployment problem for IEEE 802.11ad network in a cabin environment.

However, since IEEE 802.11ad is limited by small coverage area, it can not completely replace but necessarily cooperate with the legacy 2.4/5GHz WLAN, i.e., IEEE 802.11a/b/g/n/ac. As illustrated in Fig. 1, in a multi-band WLAN [19]–[27], 2.4/5GHz and 60GHz bands coexist with different coverage area due to distinct propagation properties. In a multi-band WLAN, two most important issues are: how and when to switchover between WiGig in 60GHz band and legacy Wi-Fi in 2.4/5GHz band. The first question has been addressed in the related work [19], [20]. In this paper, we focus on the second question, in which the key point is to detect or predict the 60GHz band coverage area in an energy efficient way.

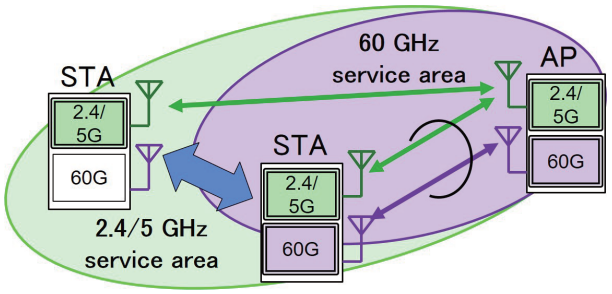

FIGURE 1. A system model of multi-band WLAN.

To achieve ultra-high data rates, connections in 60GHz band is always preferred if it is available. However, due to the propagation characteristics of different frequencies, the coverage area of 60GHz band is generally smaller than that of 2.4/5GHz band. To detect the available band in a given location, the end device needs to sense the multiple bands continuously. Obviously, this sensing operation needs to keep the RF units on and listening the beacon from the access point all the time, which results in substantial energy consumption overhead. To save the energy consumption, the existing work [25]–[27] has proposed to predict the 60GHz WLAN coverage area based on the signal strength in 2.4/5GHz band, e.g., by using RSSI (Received Signal Strength Indicator). In this work, however, we demonstrate that the prediction error of the existing approaches could be large in indoor environment, especially in relatively small rooms where strong reflected waves exist.

To solve the aforementioned issues, in this paper, we propose an energy efficient learning-based indoor multi-band WLAN system for smart buildings, in which the end device predicts the 60GHz band coverage area by learning the size and materials of the building. As the multi-path propagation could degrade the accuracy of the prediction, we introduce time, space and frequency diversities to improve the reliability. Extensive experiments are carried out in indoor environment and the evaluation results demonstrate that the proposal outperforms the existing schemes in terms of accuracy. Moreover, the key design factors in our system, i.e., margin of the threshold, forgetting coefficient, measurement interval and time diversity branches, are intensively evaluated and analyzed. The key contributions of this paper are summarized as follows.

- We propose an energy efficient learning-based indoor multi-band WLAN system for smart buildings, which could adapt to diverse indoor environment.
- To combat the negative effect of multiple reflected waves in the building, time, space and frequency diversities are all utilized and intensively evaluated.
- Based on experiments, the key design parameters are analyzed, and extensive evaluation results show that the proposal outperforms the existing approach substantially.

The rest of the paper is organized as follows. We introduce the generic 60GHz band detection method and its associated problems in Section II. In Section III, we present the proposed framework, learning mechanism and a novel RSSI measurement method. In Section IV, we present the experimental settings and evaluation results. We conclude this paper in Section V.

II. 60GHZ BAND DETECTION IN MULTI-BAND WLAN

A. RSSI-BASED 60GHZ BAND DETECTION METHOD

As illustrated in Fig. 1, the access point and STA (mobile station) of multi-band WLAN need to equipt RF units for both 2.4/5GHz and 60GHz bands. Generally, the coverage area of 2.4/5GHz band is much larger than that of 60GHz band. Therefore, it is reasonable to assume that at a given location, if the STA could communicate with access point through 60GHz band, then the communication in 2.4/5GHz band is also available. For a multi-band WLAN STA, if its RF units for 2.4/5GHz and 60GHz bands are always on, then it can easily check the available bands based on the status of the received beacon from access point. However, this continuous scanning operation leads to substantial energy consumption overhead, especially when the STA is operating outside the coverage area of 60GHz band.

To save the energy, a straightforward solution is to turn on the 60GHz RF unit only when the communications in 60GHz band is available. To this end, the existing work [25], [26] proposed to predict the 60GHz band coverage area by utilizing the signal strength from 2.4/5GHz band. Specifically, access point sends the beacon through 2.4/5GHz band to STA periodically. And STA checks the RSSI of the beacon, and initiates the 60GHz band transmission if the RSSI is larger than a threshold.

In the following part, we derive the relationship of received signal power between 2.4/5GHz band and 60GHz band in an indoor WLAN environment. For the signal propagation in 60GHz band, the direct wave dominates, since the transceiver in 60GHz uses directional antenna. The received power P_{r60G}

could be expressed as

$$P_{r60G} = P_{t60G} G_{t60G} G_{r60G} \left(\frac{\lambda_{60G}}{4\pi r_0}\right)^2, \quad (1)$$

where P_{t60G} is the transmitting power, G_{t60G} and G_{r60G} are the transceiver antenna gains, λ_{60G} is wavelength and r_0 is the traveling distance of the direct wave (distance between transceiver antennas). On the other hand, for the signal propagation in 2.4/5GHz band, multiple reflected waves exist besides the direct wave, since the transceiver uses omnidirectional antenna. In general, the instantaneous electric field strength could be expressed as

$$E_r(t) = \sum_{m=0}^{k} A_m e^{j\omega(t-\tau_m)}, \quad (2)$$

where A_m is the amplitude of received signal from $n-$th propagation path, τ_m is the delay of received signal from $n-$th propagation path and k is the number of reflected waves. Noted that $m = 0$ is the direct wave, and $m \geq 1$ are the reflected waves. Therefore, the instantaneous received power is

$$\begin{aligned} P &= \frac{1}{2} E_r(t) E_r(t)^* \\ &= \sum_{m=0}^{k} \frac{A_m^2}{2} + \sum_{m=0}^{k} \sum_{n=0}^{k} A_m A_n e^{j\omega(\tau_n - \tau_m)} m \neq n \\ &= \sum_{m=0}^{k} \frac{A_m^2}{2} + \sum_{m=0}^{k} \sum_{n=0}^{k} 2A_m A_n \cos\omega(\tau_n - \tau_m) m > n, \end{aligned} \quad (3)$$

where the second terms is a variant part, which could be averaged to 0 if enough samples are taken. Based on Eqn. (3), we could express the received power in 2.4/5GHz band as

$$P_{r2.4/5G} = P_{t2.4/5G} G_{t2.4/5G} G_{r2.4/5G} \left(\sum_{m=0}^{k} \left(\frac{\lambda_{2.4/5G}}{4\pi r_m}\right)^2 R_m^2\right), \quad (4)$$

where $P_{t2.4/5G}$ is the transmitting power, $G_{t2.4/5G}$ and $G_{r2.4/5G}$ are the transceiver antenna gains, $\lambda_{2.4/5G}$ is the wavelength, and R_m denotes the reflection coefficient. In a LOS (Line Of Sight) environment, it is reasonable to assume that

$$\left(\frac{\lambda_{2.4/5G}}{4\pi r_0}\right)^2 \gg \left(\frac{\lambda_{2.4/5G}}{4\pi r_m}\right)^2 R_m^2. \quad (5)$$

Therefore, Eqn. (4) could be approximated as

$$P_{r2.4/5G} \cong P_{t2.4/5G} G_{t2.4/5G} G_{r2.4/5G} \left(\frac{\lambda_{2.4/5G}}{4\pi r_0}\right). \quad (6)$$

Finally, based on Eqns. (1) and (6), the received power in 60GHz band could be estimated by that in 2.4/5GHz band as

$$P_{r60G} = P_{r2.4/5G} \frac{\lambda_{60G}^2 P_{t60G} G_{t60G} G_{r60G}}{\lambda_{2.4/5G}^2 P_{t2.4/5G} G_{t2.4/5G} G_{r2.4/5G}}. \quad (7)$$

To average the variant term in Eqn. (3), multiple received signals from different receiving status are required. To this end, diversity techniques, e.g., space diversity and time diversity, are widely utilized. Space diversity, also known as antenna diversity, uses two or more antennas to improve the quality and reliability of a wireless link. Currently, most of the WLAN access point are equipped with more than two antennas. And to obtain time diversity, the moving STA could combine the received signals from different locations.

B. PROBLEMS IN EXISTING 60GHZ BAND DETECTION METHOD

The aforementioned 60GHz band detection method assumes that both 2.4/5GHz and 60GHz band signals follow the free space path loss characteristics. However, the propagation characteristic for transmission in 2.4/5GHz in an indoor environment may not follow the free space path loss model, due to the multiple strong reflected waves from the walls and ceiling. To verify this argument, we have performed experiments (as shown in Fig. 2) in different indoor environments, i.e., a conference room with the size of 11m×16m×2.8m, and an auditorium with the size of 34m×22m×7.5m. We use an IEEE 802.11n WLAN with central frequency 5.32GHz, number of subcarrier 56, subcarrier spacing 312.5KHz, and transmitting power 180mW. We consider that the space diversity branch is 3, and set the access point's antenna height at 1.8m, 2.0m and 2.2m. For conference room scenario, we measured total 1275 receiver points, in range 5m ×10.2m with 0.2m spacing. For auditorium scenario, we measured total 1922 receiver points, in range 6.2m ×12.4m with 0.2m spacing. The used experimental equipments are summarized in Table 1.

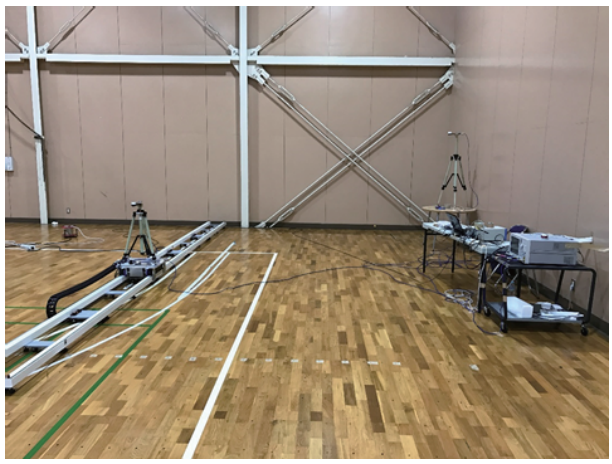

FIGURE 2. Image of the performed experiment.

Fig. 3 shows the experiment results for conference room, i.e., a relative small indoor environment. As illustrated in Fig. 3(a), we could find out that the the measured path loss is smaller than the free space path loss model, due to the existence of multiple strong reflected waves. And Fig. 3(b) gives a direct image of the received signal power's

TABLE 1. Equipments in experiment.

Hardware	Manufacturer	Product
Network analyzer	agilent	E5071C
Dipole antenna	Antenna Giken	ASD5650B
Positioner	DEVICE	DT3131HAVI/O
Antenna fixed tripod	DEVICE	AE00-19A
Computer	DELL	Inspiron

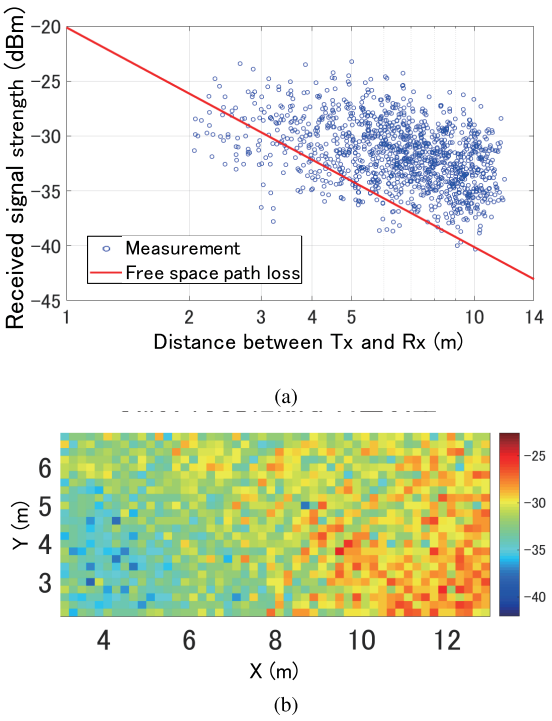

FIGURE 3. Experiment results in conference room. (a) Received signal strength versus Tx-Rx distance. (b) 2-D distribution of received signal strength.

2-D distribution. We could observe that many spots that are far away from the access point has higher received power level than the closed ones. On the other hand, Fig. 4 shows the experiment results for the auditorium, i.e., a relative large indoor environment. As illustrated in Figs. 4(a) and 4(b), we could observe that the free space path loss characteristic basically holds for 5GHz WLAN.

Based on these experiment results, we argue that the path loss characteristic in an indoor 2.4/5GHz WLAN would vary according to the size of the room. Therefore, utilizing 2.4/5GHz RSSI to predict the 60GHz coverage area directly may result in poor accuracy. An environment-aware prediction method is required.

III. PROPOSED ENERGY EFFICIENT LEARNING-BASED 60GHZ BAND COVERAGE PREDICTION MECHANISM

A. PROPOSED FRAMEWORK

To solve the aforementioned problems, we propose an energy efficient 60GHz band coverage prediction mechanism by utilizing learning mechanism [28]–[30] in this paper. We consider an indoor multi-band WLAN with access point and

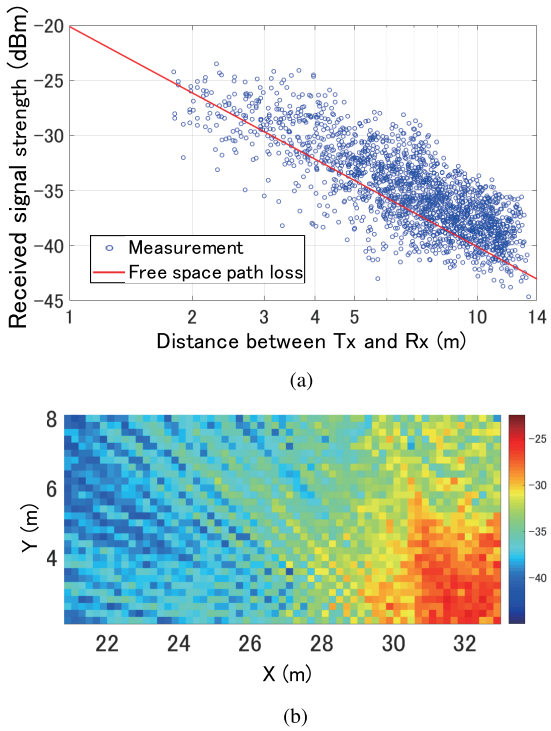

FIGURE 4. Experiment results in auditorium. (a) Received signal strength versus Tx-Rx distance. (b) 2-D distribution of received signal strength.

mobile STA that could communicate in both 2.4/5GHz and 60GHz bands. The proposed mechanism collects multiple sets of RSSI data from 2.4/5GHz and 60GHz signals, and dynamically learns a *correlation coefficient* according to the current indoor environment. Based on this correlation coefficient and RSSI of 2.4/5GHz, we predict the 60GHz coverage area. To save the energy consumption, the RF unit for 60GHz band turns on only when the current location is predicted to be located inside the 60GHz coverage.

Fig. 5 illustrates the flow chart of the proposed mechanism. Specifically, access point continuously sends beacon by using 2.4/5GHz band, in which the learned correlation coefficient is involved. STA keeps the 2.4/5GHz RF unit on, receives the beacon from access point and measures its RSSI. Based on the 2.4/5GHz RSSI and correlation coefficient, STA predicts the 60GHz RSSI at current location. If the predicted 60GHz RSSI is lower than a *threshold*, the STA considers that currently it is outside the 60GHz band coverage area, and thus keeps the 60GHz RF unit off to save energy. Otherwise, the STA considers that the connection in 60GHz band is available, and thus turns on its 60GHz RF unit to pursue ultra-high speed transmission. After that, the STA simultaneously measures the RSSI of both 2.4/5GHz and 60GHz, and sends back these information to the access point. Upon these information, the access point learns and updates the correlation coefficient accordingly, and encapsulates it in the next beacon as the feedback to STA.

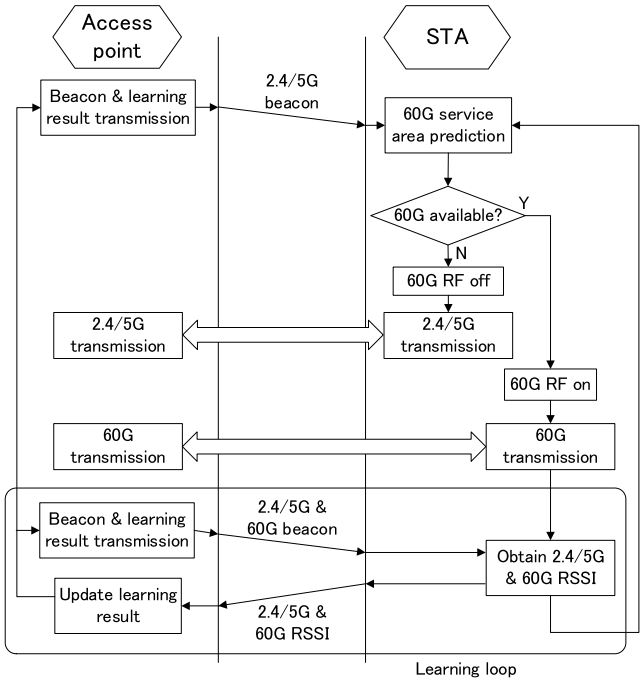

FIGURE 5. Flow chart of the proposed mechanism.

B. LEARNING MECHANISM

Based on Friis' transmission equation, the RSSI of 2.4/5GHz signal can be expressed as

$$RSSI_{2.4/5G} = P_t + G_{t/r} + 20\log_{10}\left(\lambda_{2.4/5G}/4\pi\right) - 10\log_{10}\left(d_i\right)^n, \quad (8)$$

where P_t is the transmitting power, $G_{t/r}$ is the transceiver antenna gain, $\lambda_{2.4/5G}$ is the 2.4/5GHz wavelength, d_i is the distance between transceiver antennas, and n is the attenuation coefficient. In Eqn. (8), the first three terms are system design parameters, which can be denoted as a constant K. Then Eqn. (8) could be rewritten as

$$RSSI_{2.4/5G} = -n \times 10\log_{10}\left(d_i\right) + K_{2.4/5G}. \quad (9)$$

Similarly, since the signal propagation in 60GHz band WLAN follows the free space path loss model with $n = 2$, we have

$$RSSI_{60G} = -2 \times 10\log_{10}\left(d_i\right) + K_{60G}. \quad (10)$$

Based on Eqns. (9) and (10), we can calculate the correlation coefficient a_i using the i-th set of 2.4/5GHz band RSSI and 60GHz band RSSI at a given location as follows.

$$a_i = \frac{RSSI_{60G} - K_{60G}}{RSSI_{2.4/5G} - K_{2.4/5G}}. \quad (11)$$

Based on the i-th measured correlation coefficient a_i, and the previous $(i-1)$-th predicted correlation coefficient A_{i-1}, we can calculate the current i-th predicted correlation coefficient as

$$A_i = (1-\eta)A_{i-1} + \eta a_i, \quad (12)$$

where η is a forgetting coefficient with range $0 \le \eta \le 1$. A_i will always use the initial value when $\eta = 0$, and use the current measured value when $\eta = 1$.

We set the initial value $A_0 = 1$ by assuming the free space path loss model. And the correlation coefficient A_i will be updated by learning the effect of reflected waves in the current indoor environment, and finally converges to some value that larger than 1. Access point will send this environment aware correlation coefficient A_i to STA for predicting the 60GHz band coverage area.

C. RSSI MEASUREMENT

As we mentioned previously, space and time diversity techniques are adopted to suppress the variance of received power. Since the 2.4/5GHz WLAN utilizes OFDM (Orthogonal Frequency Division Multiplexing) to transmit data, we intend to further mitigate the received power variance by obtaining frequency diversity. Specifically, the average power (AP) method which calculates the average power of all subcarriers and, the peak power (PP) method which utilizes the maximum power spectrum in all subcarriers are investigated. Noted that the normal RSSI measurement method is equivalent to AP method.

Considering multiple reflected waves, the normalized impulse response $h(t)$ and corresponding transfer function $T(f)$ could be expressed as follows.

$$h(t) = \rho_0\delta(t) + \sum_{k=1}^{N-1}\rho_k\delta(t-\tau_k), \quad (13)$$

$$T(f) = \rho_0 + \sum_{k=1}^{N-1}\rho_k e^{-j\omega(t-\tau_k)}, \quad (14)$$

where $\delta(t)$ is delta function, ρ is relative strength, and N is the number of direct wave and reflected waves. Based on Eqn. (14), the received signal strength by AP and PP methods could be calculated as follows, respectively.

$$P_{average} = \frac{1}{M}\sum_{i=0}^{M-1}\left(|T(f_i)|^2\right), \quad (15)$$

$$P_{peak} = \max_{0\le i\le M-1}\left(|T(f_i)|^2\right), \quad (16)$$

where M is the sampling number.

Fig. 6 illustrates the correlation between 2.4/5GHz RSSI and 60GHz RSSI, which is based on our experiment results in the conference room scenario with space diversity branch 3. The approximation line is calculated by using Eqn. (11). Specifically, a_i is calculated from all the pairs of 2.4/5GHz and 60GHz RSSI data by using least squares method. The standard deviation of 2.4/5GHz RSSI, and the RMS (Root Mean Square) of error between 60GHz RSSI and estimation line are summarized in Table 2. We find out that PP method outperforms AP method in terms of achieving low variance in 2.4/5GHz RSSI, and thus low estimation error for 60GHz RSSI. The reason is that the AP method cannot suppress the variance of received power when there exists strong

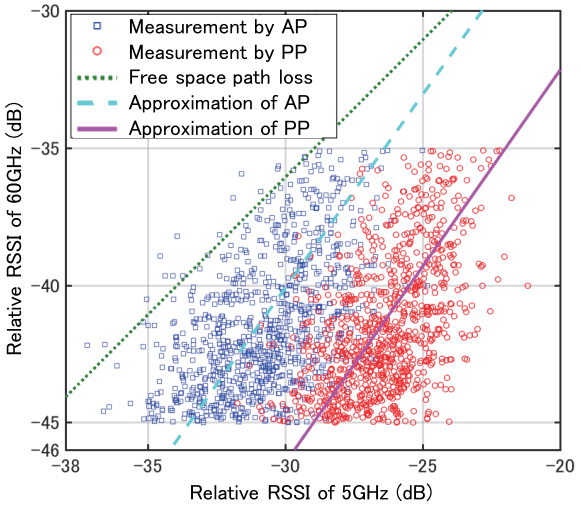

FIGURE 6. Correlation between 2.4/5GHz RSSI and 60GHz RSSI by different RSSI measurement methods.

TABLE 2. Standard deviation of 2.4/5GHz RSSI & RMS of error between 60GHz RSSI and estimation line.

Measurement method	Standard deviation	RMS (dB)
AP	1.99	2.62
PP	1.68	2.41

TABLE 3. Average and median of 2.4/5GHz RSSI.

Measurement method	Average (dB)	Median (dB)
AP	-30.33	-30.68
PP	-26.06	-26.33
(Difference)	4.27	4.35

reflected wave with relatively small delay. However, compared to AP method, PP method tends to be biased towards the high RSSI value. Therefore, a compensation K_{OFFSET} is required to be added to parameter $K_{2.4/5G}$, when we estimate the 60GHz RSSI using Eqn. (11). Based on the average and median value of 2.4/5GHz RSSI shown in Table 3, we use $K_{OFFSET} = 4.3$dB in the following parts for PP method.

IV. EXPERIMENTS

A. EXPERIMENTAL SETTINGS

To evaluate the performance of the proposed mechanism, we use the similar experimental settings in Section II-B. Specifically, experiments are performed in two indoor environments with different sizes, i.e., a conference room with the size of 11m×16m×2.8m, and an auditorium with the size of 34m×22m×7.5m.

To combat the multipath fading, space, time and frequency diversity techniques are all considered. To obtain space diversity gain, we use the access point with 3 antennas and the heights are set to 1.8m, 2.0m and 2.2m. For the time diversity, we adopt the mobility model for the end-user as shown in Fig. 7. In generally, the user moves in a room with some purposes. Therefore, we assume the STA has several

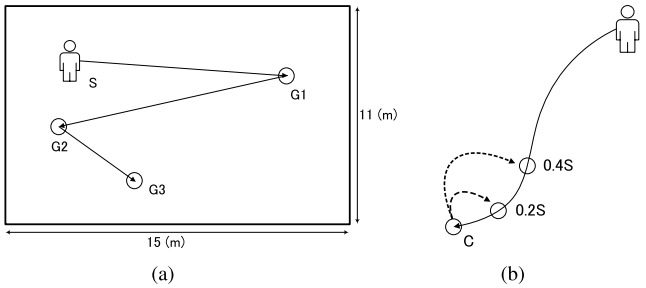

FIGURE 7. Mobility model of the end user. (a) Mobility model. (b) Time diversity with branches = 3.

destinations, and moves from the current location to the destinations by the shortest path sequentially. For instance, as shown in Fig. 7(a), STA moves from the current location S to destinations G1, G2, G3 one after another. Based on this mobility model, the time diversity gain is obtained by using the RSSI from past locations. For instance, in Fig. 7(b), STA moves with 1.0m/s, and the RSSI is recorded every 0.2s. Assuming the time diversity branch is set to 3, then the RSSI of the current location C is calculated by averaging that of 3 locations, i.e., current location, location of 0.2s ago, and location of 0.4s ago. For the frequency diversity, we measure the RSSI by using both AP and PP methods that introduced in Section III-C.

For the learning algorithm, we use the 2.4/5GHz band beacon data whose relative RSSI is below −35dB, with the purpose of avoiding the influence of directivity in the vertical plane of the dipole antenna when the RSSI is higher than −35dB. In addition, we assume that the communication in 60GHz band is available when its signal strength is larger than a given threshold, which is set to −45dB. Other experimental setting parameters are summarized in Table 4.

B. EVALUATION RESULTS

In this section, we evaluate the impacts of some key parameters of the proposed mechanism, and compare it with the existing scheme that without learning.

TABLE 4. Experimental settings.

Parameters	Values
Center frequency of 2.4/5GHz band	5.32GHz
Transmitting power in 2.4/5GHz band	180mW
Antenna gain in 2.4/5GHz band	2.15dBi
Center frequency of 60GHz band	60GHz
Transmitting power in 60GHz band	10mW
Antenna gain in 60GHz band	16dBi

1) SERVICE AREA PREDICTION

Firstly, we use Fig. 8 to illustrate the 60GHz band service area prediction by utilizing the received signal strength of 2.4/5GHz. Based on the intersection of 60GHz $RSSI = -45dB$ line and prediction line that obtained by learning, we could divide the predicted 60GHz band service

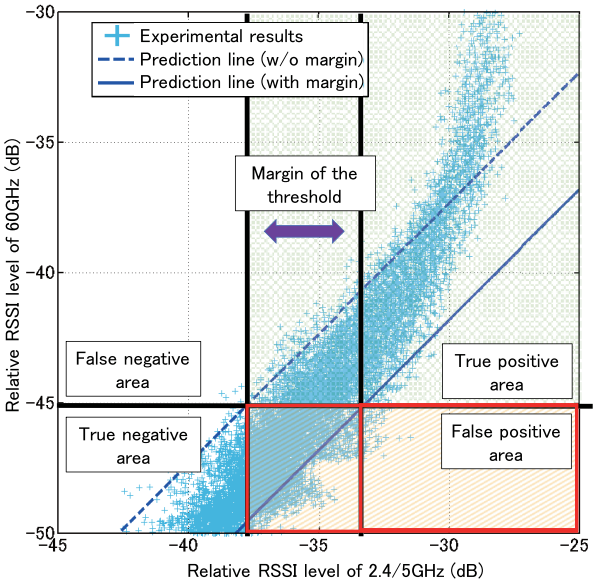

FIGURE 8. 60GHz band service area prediction.

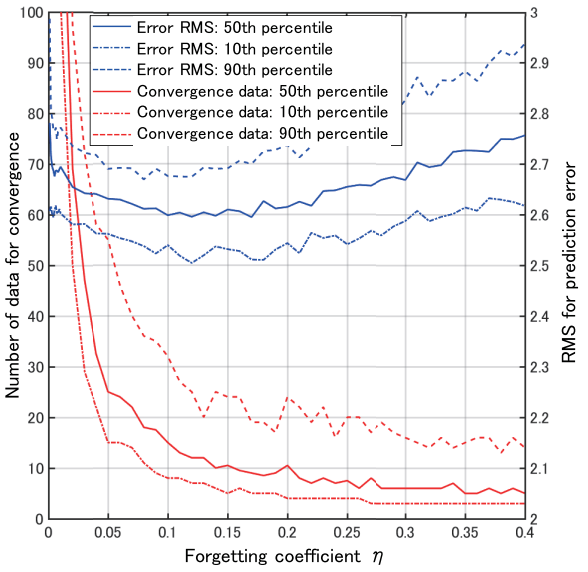

FIGURE 9. The impacts of forgetting coefficient on convergence time and prediction error by using AP method.

area into 4 areas. Specifically, we have *false negative area* that the 60GHz communication prediction result is unavailable while in fact it is available; *true positive area* that the prediction result is correct about the 60GHz communication is available; *true negative area* that the prediction result is correct about the 60GHz communication is unavailable; and *false positive area* that the prediction results is available while in fact it is not. Obviously, false positive area results in additional energy consumption which is the case that we try to avoid. To save the energy consumption, as shown in Fig. 8, we set a *margin of threshold* to reduce the false positive area. However, the false negative area increases as the margin of threshold rises. Therefore, there is a tradeoff between the 60GHz band communication opportunity and energy consumption overhead saving.

2) IMPACTS OF FORGETTING COEFFICIENT

In the proposed learning based mechanism, the forgetting coefficient η affects both the convergence time and RSSI prediction error substantially. We try to find the optimal forgetting coefficient η for the learning mechanism. Fig. 9 illustrates the impacts of η on the needed number of data for convergence, and RMS of prediction error. The convergence is defined as the status that the correlation coefficient A_i's variance is smaller than 7.7% of the convergence value when error's RMS equals 0.5dB. Noted that this result is based on the space diversity with branch 3, and normal AP method for measuring RSSI.

From the result we find that as η rises, the 60GHz band RSSI prediction error's RMS increases, however, the required number of data for convergence reduces, i.e., convergence time is shortened. On the contrary, small η leads to large number of data for convergence but better RMS of prediction error. Therefore, we could conclude that there exists a tradeoff for convergence speed and prediction accuracy. In order to achieve low prediction error at fast convergence speed, it is reasonable to set η in range $0.1 \leq \eta \leq 0.2$. In the following evaluation parts, the forgetting coefficient η is set to 0.15. Moreover, the prediction error increases sharply when $\eta < 0.1$, the reason is that within the simulation time, the defined convergence status is reached but the convergence value cannot converge to a constant.

3) IMPROVEMENT OF PP MEASUREMENT METHOD

As we introduced in Section III-C, besides the normal AP method to measure the RSSI, we propose PP method which has the potential to suppress the variance of multiple received signal power. Fig. 10 shows the evaluation results in terms of convergence time and prediction error by using PP method. Similar to Fig. 9, large forgetting coefficient leads to short convergence time but large prediction error's RMS. Compared to the results of using AP method in Fig. 9, PP method could substantially reduce the prediction error's RMS, and meanwhile, maintain the convergence speed level.

4) IMPACTS OF TIME DIVERSITY

Next, we investigate the impacts of time diversity when the STA moves randomly in the indoor environment. As shown in Fig. 11, we can observe that the variance trend of convergence data is not evident as the time diversity branch and RSSI measurement interval change. Therefore, we can conclude that the convergence time of the learning scheme is irrelevant to either the time diversity branches or time interval of RSSI measurement, and it is only affected by forgetting coefficient. In addition, by comparing the results in Figs. 11(a) and 11(b), we find out that PP method still

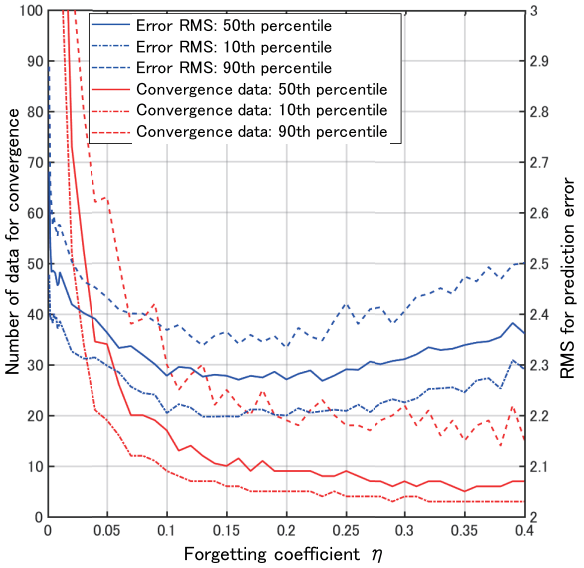

FIGURE 10. The impacts of forgetting coefficient on convergence time and prediction error by using PP method.

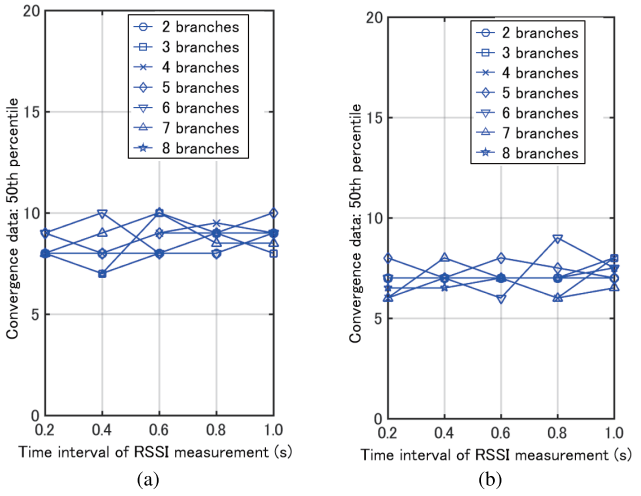

FIGURE 11. Convergence data versus time interval of RSSI measurement: 50th percentile. (a) AP method. (b) PP method.

slightly outperforms AP method in terms of convergence data in the mobile STA scenario.

Furthermore, we investigate the variance of 60GHz band RSSI prediction error's RMS with different time diversity branches and RSSI measurement time interval. From Fig. 12, we find out generally, for the same time diversity, the prediction error increases as the RSSI measurement time interval rises, due to the used RSSI data is measured from the locations that are far away from the current one. And the optimal RSSI measurement time interval changes at different time diversity branches. Specifically, it would be appropriate to set the time interval at 0.4s for diversity branches 2 and 3, and 0.2s for diversity branches that are higher than 4. And the minimum prediction error is achieved at RSSI measurement

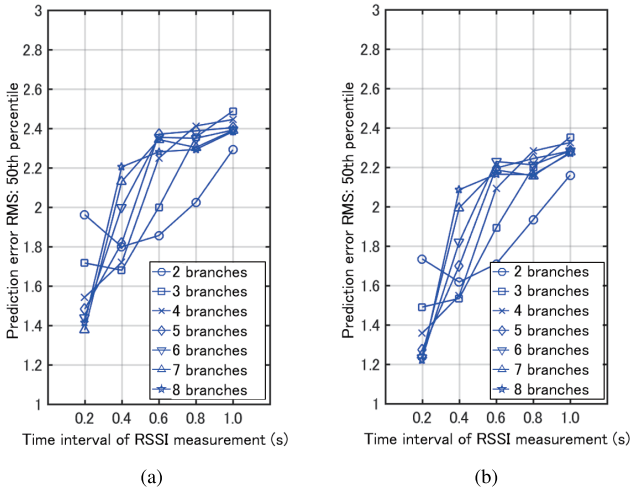

FIGURE 12. 60GHz band RSSI prediction error's RMS versus time interval of RSSI measurement: 50th percentile. (a) AP method. (b) PP method.

time interval 0.2s with time diversity branches 7. Similar to the results of convergence data, PP method slightly outperforms AP method also in terms of prediction error as shown in Figs. 12(a) and 12(b).

5) FALSE POSITIVE RATE

Fig. 13 compares the proposed approach with the existing method (without learning) with space diversity branch 3. We investigate the relationship between false positive rate and margin of threshold. As expected, as the margin of threshold increases, the false positive rate for both approaches could be reduced. However, increasing the margin of threshold leads to the loss of 60GHz band usage opportunities, which is the scenario that we try to avoid. From Fig. 13, we could observe that compared to the existing scheme, the proposed learning-based approach is able to reduce the margin of threshold from 7.4dB and 7.9dB to 0.1dB and 0.6dB, respectively, when the required false positive rates are 0.05 and 0.02. In addition, almost the same improvement could be observed for both the

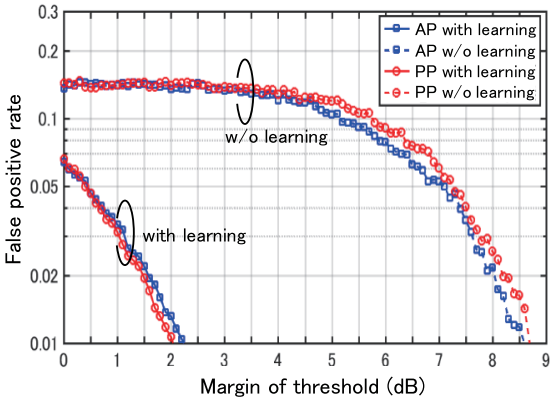

FIGURE 13. Comparison between proposal and existing scheme in terms of false positive rate and margin of threshold.

AP and PP methods, which implies that the improvement by learning mechanism on false positive rate is not sensitive to the RSSI measurement method.

Finally, Fig. 14 illustrates the false positive rate of the proposed scheme with changing RSSI measurement time interval, when both the space and time diversities are considered. It is straightforward that the false positive rate decreases as the measurement time interval becomes larger, since the RSSI data are collected from the locations that are far from the current one. And we find out that increasing the time diversity branch cannot improve the false positive rate significantly. For both settings, i.e., false positive rates equal 0.05 and 0.02, the PP method outperforms AP method by achieving low false positive rate.

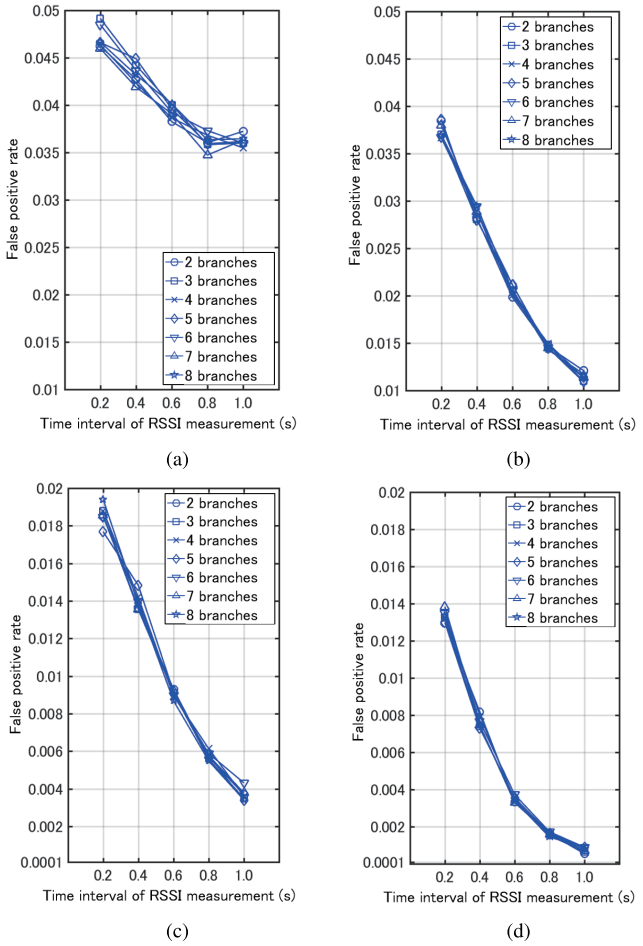

FIGURE 14. False positive rate variance versus RSSI measurement time interval. (a) AP method with false positive rate 0.05. (b) PP method with false positive rate 0.05. (c) AP method with false positive rate 0.02. (d) PP method with false positive rate 0.02.

V. CONCLUSIONS

In this paper, we have proposed an energy efficient learning-based indoor multi-band WLAN system for smart buildings. The proposed mechanism could adapt to different indoor environment by learning the influences of reflected waves. To eliminate the negative effect of multiple reflected waves, we propose PP method to measure the RSSI value instead of the traditional AP method. We have performed extensive experiments to evaluate the effects of key design parameters in our mechanism, e.g., forgetting coefficient, time diversity branch and measurement time interval. The evaluation results demonstrate that compared to existing scheme, the proposed mechanism could reduce the margin of threshold by 7.3dB at the same false positive rate requirement, which leads to a substantially reduced 60GHz band usage opportunity wastage.

REFERENCES

[1] H. Jiang, C. Cai, X. Ma, Y. Yang, and J. Liu, "Smart home based on WiFi sensing: A survey," *IEEE Access*, vol. 6, pp. 13317–13325, 2018.
[2] M. Gao, K. Wang, and L. He, "Probabilistic model checking and scheduling implementation of an energy router system in energy Internet for green cities," *IEEE Trans. Ind. Informat.*, vol. 14, no. 4, pp. 1501–1510, Apr. 2018.
[3] X. He, K. Wang, H. Huang, and B. Liu, "QoE–driven big data architecture for smart city," *IEEE Commun. Mag.*, vol. 56, no. 2, pp. 88–93, Feb. 2018.
[4] K. Wang *et al.*, "A survey on energy Internet: Architecture, approach, and emerging technologies," *IEEE Syst. J.*, pp. 1–14, Jan. 2017.
[5] K. Wang, H. Li, Y. Feng, and G. Tian, "Big data analytics for system stability evaluation strategy in the energy Internet," *IEEE Trans. Ind. Informat.*, vol. 13, no. 4, pp. 1969–1978, Aug. 2017.
[6] H. Jiang, K. Wang, Y. Wang, M. Gao, and Y. Zhang, "Energy big data: A survey," *IEEE Access*, vol. 4, pp. 3844–3861, Aug. 2016.
[7] C. J. Hansen, "WiGig: Multi-gigabit wireless communications in the 60 GHz band," *IEEE Wireless Commun.*, vol. 18, no. 6, pp. 6–7, Dec. 2011.
[8] *IEEE Standard for Information Technology—Telecommunications and Information Exchange Between Systems—Local and Metropolitan Area Networks—Specific Requirements—Part 11: Wireless Lan Medium Access Control (MAC) and Physical Layer (PHY) Specifications Amendment 3: Enhancements for Very High Throughput in the 60 GHz Band*, IEEE Standard 802.11ad-2012 (Amendment to IEEE Standard 802.11-2012, as amended by IEEE Standard 802.11ae-2012 IEEE Standard 802.11aa-2012), Dec. 2012, pp. 1–628.
[9] T. Wang, M. Umehira, H. Otsu, S. Takeda, T. Miyajima, and K. Kagoshima, "A twin cylinder model for moving human body shadowing in 60 GHz wlan," in *Proc. 21st Asia–Pacific Conf. Commun. (APCC)*, Oct. 2015, pp. 188–192.
[10] Y. Koda, K. Yamamoto, T. Nishio, and M. Morikura, "Time series measurement of IEEE 802.11ad signal power involving human blockage with HMM-based state estimation," in *Proc. IEEE 86th Veh. Technol. Conf. (VTC-Fall)*, Sep. 2017, pp. 1–5.
[11] M. N. U. Rajan and A. V. Babu, "Theoretical maximum throughput of IEEE 802.11ad millimeter wave wireless LAN in the contention based access period: With two level aggregation," in *Proc. Int. Conf. Wireless Commun., Signal Process. Netw. (WiSPNET)*, Mar. 2017, pp. 2531–2536.
[12] O. Semiari, W. Saad, M. Bennis, and M. Debbah, "Performance analysis of integrated sub-6 GHz-millimeter wave wireless local area networks," in *Proc. IEEE Global Commun. Conf. (GLOBECOM)*, Dec. 2017, pp. 1–7.
[13] H. Kushida, H. Mano, M. Takai, Z. Liu, and S. Ishihara, "On the effectiveness of fils in IEEE 802.11ad wireless networks," in *Proc. 23rd Asia–Pacific Conf. Commun. (APCC)*, Dec. 2017, pp. 1–6.
[14] E. Kurniawan, L. Zhiwei, and S. Sun, "Machine learning-based channel classification and its application to IEEE 802.11ad communications," in *Proc. IEEE Global Commun. Conf. (GLOBECOM)*, Dec. 2017, pp. 1–6.
[15] S. K. Saha, V. V. Vira, A. Garg, A. Tennenbaum, and D. Koutsonikolas, "On the feasibility of indoor IEEE 802.11ad WLANs," in *Proc. IEEE Conf. Comput. Commun. Workshops (INFOCOM WKSHPS)*, Apr. 2015, pp. 107–108.
[16] S. K. Saha, A. Garg, and D. Koutsonikolas, "A first look at TCP performance in indoor IEEE 802.11ad WLANs," in *Proc. IEEE Conf. Comput. Commun. Workshops (INFOCOM WKSHPS)*, Apr. 2015, pp. 63–64.
[17] T. Yamada, T. Nishio, M. Morikura, and K. Yamamoto, "Experimental evaluation of IEEE 802.11ad millimeter-wave WLAN devices," in *Proc. 21st Asia–Pacific Conf. Commun. (APCC)*, Oct. 2015, pp. 278–282.
[18] Q. Chen, P. H. Tan, Z. Lin, S. Sun, and W. Zhao, "Design and optimization of IEEE 802.11ad-based dense network in cabin environment," in *Proc. IEEE Global Commun. Conf. (GLOBECOM)*, Dec. 2017, pp. 1–6.

[19] K. Nguyen, M. G. Kibria, K. Ishizu, and F. Kojima, "Feasibility study of providing backward compatibility with MPTCP to WiGig/IEEE 802.11 ad," in *Proc. IEEE 86th Veh. Technol. Conf. (VTC-Fall)*, Sep. 2017, pp. 1–5.
[20] Y. Li, C. Li, W. Chen, C. Yeh, and K. Wang, "Enabling seamless WiGig/WiFi handovers in tri-band wireless systems," in *Proc. IEEE 25th Int. Conf. Netw. Protocols (ICNP)*, Oct. 2017, pp. 1–2.
[21] Z. M. Fadlullah *et al.*, "Multi-hop wireless transmission in multi-band WLAN systems: Proposal and future perspective," *IEEE Wireless Commun.*, pp. 1–6, Oct. 2017.
[22] S. K. Dhakad, U. Dwivedi, and T. Bhandari, "Design and analysis of reconfigurable antenna using PIN diodes for multi band WLAN applicaions," in *Proc. Int. Conf. Wireless Commun., Signal Process. Netw. (WiSPNET)*, Mar. 2017, pp. 1705–1708.
[23] T. Motegi, T. Miyajima, M. Umehira, and S. Takeda, "Further evaluation of frequency cooperative ARQ scheme for multi-band WLAN," in *Proc. 15th Int. Symp. Commun. Inf. Technol. (ISCIT)*, Oct. 2015, pp. 97–100.
[24] R. Teng, K. Yano, and T. Kumagai, "A distributed-and-interactive reporting scheme for collective-sensing in multi-band wireless LAN system," in *Proc. 20th Int. Symp. Wireless Pers. Multimedia Commun. (WPMC)*, Dec. 2017, pp. 154–160.
[25] S. Wada, M. Umehira, S. Takeda, T. Miyajima, and K. Kagoshima, "Energy efficient RSSI-based 60 GHz WLAN discovery for multi-band WLAN," in *Proc. 20th Asia–Pacific Conf. Commun. (APCC)*, Oct. 2014, pp. 30–35.
[26] M. Umehira, G. Saito, S. Wada, S. Takeda, T. Miyajima, and K. Kagoshima, "Feasibility of RSSI based access network detection for multi-band WLAN using 2.4/5 GHz and 60 GHz," in *Proc. Int. Symp. Wireless Pers. Multimedia Commun. (WPMC)*, Sep. 2014, pp. 243–248.
[27] S. K. Saha, V. V. Vira, A. Garg, and D. Koutsonikolas, "Multi-Gigabit indoor WLANs: Looking beyond 2.4/5 GHz," in *Proc. IEEE Int. Conf. Commun. (ICC)*, May 2016, pp. 1–6.
[28] R. Thapa, L. Jiao, B. J. Oommen, and A. Yazidi, "A learning automaton-based scheme for scheduling domestic shiftable loads in smart grids," *IEEE Access*, vol. 6, pp. 5348–5361, 2018.
[29] X. He, K. Wang, H. Huang, T. Miyazaki, Y. Wang, and S. Guo, "Green resource allocation based on deep reinforcement learning in content-centric IoT," *IEEE Trans. Emerg. Topics Comput.*, pp. 1–15, Feb. 2018.
[30] K. Wang *et al.*, "Wireless big data computing in smart grid," *IEEE Wireless Commun.*, vol. 24, no. 2, pp. 58–64, Apr. 2017.

XIAOYAN WANG (S'11–M'14) received the B.E. degree from Beihang University, China, and the M.E. and Ph.D. degrees from the University of Tsukuba, Japan. He was an Assistant Professor (by special appointment) with the National Institute of Informatics, Japan, from 2013 to 2016. He is currently an Assistant Professor with the Graduate School of Science and Engineering, Ibaraki University, Japan. His research interests include networking, wireless communications, cloud computing, big data, security, and privacy.

MASAHIRO UMEHIRA (M'85) received the B.E., M.E., and Ph.D. degrees from Kyoto University, Kyoto, Japan, in 1978, 1980, and 2000, respectively. Since joining Nippon Telegraph and Telephone Corporation in 1980, he has been engaged in the research and development of modem and TDMA equipment for satellite communications, TDMA satellite communication systems, broadband wireless access systems for mobile multimedia services, and ubiquitous wireless systems. From 1987 to 1988, he was with the Communications Research Center, Department of Communications, Canada, as a Visiting Scientist. Since 2006, he has been a Professor with Ibaraki University, Ibaraki, Japan. His research interests include broadband wireless access technologies, wireless networking, cognitive radio, future satellite communication systems, and wireless-based ubiquitous systems. He received the Young Engineer Award and the Achievement Award from IEICE in 1987 and 1999, respectively. He also received the Education, Culture, Sports, Science and Technology Minister Award in 2001 and the TELECOM System Technology Award from the Telecommunications Advancement Foundation in 2003.

HIROYUKI OTSU received the B.E. and M.E. degrees from Ibaraki University, Ibaraki, Japan, in 2014 and 2016, respectively. He is currently an Engineer with Mitsubishi Electric Corporation Energy System Center. His research interests include broadband WLAN, learning mechanism, and cognitive radio.

TAKYUYA KAWATANI received the B.E. degree from Ibaraki University, Ibaraki, Japan, in 2017. He is currently an Engineer with KYOWA EXEO Corporation. His research interests include broadband WLAN, learning mechanism, and cognitive radio.

SHIGEKI TAKEDA (M'00) received the B.E., M.E., and D.E. degrees in electrical and electronic engineering from Tottori University, Tottori, Japan, in 1996, 1998, and 2000, respectively. Since 2000, he has been with the Graduate School of Science and Engineering, Ibaraki University, Ibaraki, Japan, where he is currently a Professor. His research interests are in RFID tag, MIMO, and adaptive array antenna.